Experimental Test of the Jarzynski Equality in a Single Spin-1 System Using High-Fidelity Single-Shot Readouts

Wenquan Liu,[1,2,4] Zhibo Niu,[1,2] Wei Cheng,[1,2] Xin Li,[5] Chang-Kui Duan,[1,2] Zhangqi Yin,[5,*] Xing Rong,[1,2,3,†] and Jiangfeng Du[1,2,3,‡]

[1]*CAS Key Laboratory of Microscale Magnetic Resonance and School of Physical Sciences, University of Science and Technology of China, Hefei 230026, China*

[2]*CAS Center for Excellence in Quantum Information and Quantum Physics, University of Science and Technology of China, Hefei 230026, China*

[3]*Hefei National Laboratory, University of Science and Technology of China, Hefei 230088, China*

[4]*School of Science, Beijing University of Posts and Telecommunications, Beijing, 100876, China*

[5]*Center for Quantum Technology Research and Key Laboratory of Advanced Optoelectronic Quantum Architecture and Measurements (MOE), School of Physics, Beijing Institute of Technology, Beijing 100081, China*

(Received 13 December 2022; revised 22 October 2023; accepted 24 October 2023; published 27 November 2023)

The Jarzynski equality (JE), which connects the equilibrium free energy with nonequilibrium work statistics, plays a crucial role in quantum thermodynamics. Although practical quantum systems are usually multilevel systems, most tests of the JE were executed in two-level systems. A rigorous test of the JE by directly measuring the work distribution of a physical process in a high-dimensional quantum system remains elusive. Here, we report an experimental test of the JE in a single spin-1 system. We realized nondemolition projective measurement of this three-level system via cascading high-fidelity single-shot readouts and directly measured the work distribution utilizing the two-point measurement protocol. The validity of the JE was verified from the nonadiabatic to adiabatic zone and under different effective temperatures. Our work puts the JE on a solid experimental foundation and makes the nitrogen-vacancy (NV) center system a mature toolbox to perform advanced experiments of stochastic quantum thermodynamics.

DOI: 10.1103/PhysRevLett.131.220401

Processes in nature usually deviate from equilibrium, but most thermodynamic principles describing nonequilibrium processes are only presented in the form of inequalities [1–3]. Although the fluctuation-dissipation theorem is valid in the close-to-equilibrium regime [4,5], an accurate description of all out-of-equilibrium processes has not been established until the proposition of the Jarzynski equality (JE) [6,7]:

$$\langle e^{-\beta W}\rangle = e^{-\beta \Delta F}. \tag{1}$$

The JE connects the equilibrium free energy difference ΔF of a system with the ensemble average of the exponentiated work $\langle e^{-\beta W}\rangle$ during a switching process at inverse temperature β. The equality is valid regardless of the speed of the switching process. Thus, the JE gives a shortcut to estimate the free energy difference between two system configurations, especially for systems whose equilibrium states and reversible processes are hardly or not accessible.

The JE has been examined in various classical systems [8–14], but its test in the quantum domain remains inadequate. The inadequacy lies in the fact that practical quantum systems usually possess many energy levels, yet most experimental tests have been limited to two-level systems [15–17]. There is one test executed in a multilevel trapped-ion system, but the work distribution was mimicked via a classical presampling method because the phonon state measurement is destructive [18]. To put the JE on a solid experimental foundation, a rigorous test that directly measures the work distribution of a physical process is still urgently needed. However, measurement of work is not easy. In fact, as one of the most basic notions of physical science, work is not an observable but corresponds to some correlation functions [19,20]. In classical systems, it can be measured by continuously tracing the displacement of the particle and the force applied to it during the switching process. This method fails in quantum scenarios as the uncertainty principle constrains our ability to precisely measure operators that do not commute. For isolated quantum systems, this problem can be addressed by the two-point measurement (TPM) protocol [21–23]. In the TPM protocol, two high-fidelity nondemolition projective measurements on the energy basis are applied before and after the switching process to determine the quantity of work. However, it is challenging to realize such projective measurements, especially for high-dimensional quantum systems. Thus, a rigorous test of the JE in a high-dimensional quantum system remains an open issue.

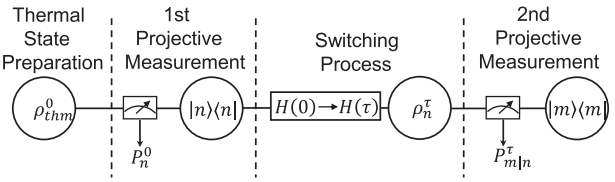

FIG. 1. Illustration of the two-point measurement protocol. First, the system is in the thermal state of the initial Hamiltonian $H(0)$. Then the system is projected into an energy eigenstate by a projective measurement. Next, the driving Hamiltonian changes from $H(0)$ to $H(\tau)$, which is called the switching process. Eventually, a second projective measurement determines the final state of the system. Work statistics of the switching process can be obtained via this protocol.

Here, we report an experimental test of the JE in a single spin-1 nuclear spin. We realized high-fidelity nondemolition projective measurement of the three-level system by cascading single-shot readouts [24]. Then the TPM protocol was implemented by performing two projective measurements of the nuclear spin that sandwich the switching process to measure the work of the process. With examinations starting from different thermal states and experiencing switching processes with different speeds, we tested the JE at different effective temperatures and in both adiabatic and nonadiabatic regions. Our results show that the JE is valid in this high-dimensional spin system.

The scheme of the TPM protocol to establish the JE is illustrated in Fig. 1. First, the Hamiltonian is $H(0)$ and the system is prepared in the thermal state $\rho^0_{\rm thm} = e^{-\beta H(0)}/Z^0$, where $Z^0 = {\rm Tr}[e^{-\beta H(0)}]$ is the partition function of the initial thermal state. Second, the first projective measurement is carried out and the system is projected to an energy eigenstate $|n(0)\rangle$ of $H(0)$ with probability $P^0_n = {\rm Tr}[\rho^0_{\rm thm}|n(0)\rangle\langle n(0)|]$. Next, the switching process is performed, while the driving Hamiltonian changes from $H(0)$ to $H(\tau)$. The state of the system becomes $\rho^\tau_n = U|n(0)\rangle\langle n(0)|U^\dagger$, where $U = \mathcal{T} e^{-i\int_0^\tau H(t)dt}$ is the evolution operator and $\mathcal{T}$ is the time-ordering operator. Finally, the second projective measurement on ρ^τ_n is applied to obtain $P^\tau_{m|n} = {\rm Tr}[\rho^\tau_n|m(\tau)\rangle\langle m(\tau)|]$, the probability of finding the system in the energy eigenstate $|m(\tau)\rangle$ of $H(\tau)$ conditioned that the evolution begins with the system in $|n(0)\rangle$. The work done on the system in the trajectory from $|n(0)\rangle$ to $|m(\tau)\rangle$ is defined as $W_{m|n} = \epsilon^\tau_m - \epsilon^0_n$ with ϵ^0_n and ϵ^τ_m being the eigenenergy of $|n(0)\rangle$ and $|m(\tau)\rangle$, respectively. Through the TPM protocol, the work distribution is obtained as

$$P(W) = \sum_{n,m} P^0_n P^\tau_{m|n} \delta(W - W_{m|n}). \tag{2}$$

Hence, the JE can be expressed as $\sum_{n,m} P^0_n P^\tau_{m|n} e^{-\beta W_{m|n}} = e^{-\beta \Delta F}$. We can then compare the exponentiated free energy difference extracted by this formula with the definition $e^{-\beta\Delta F} = [{\rm Tr}(e^{-\beta H(\tau)})/{\rm Tr}(e^{-\beta H(0)})]$ to test the JE.

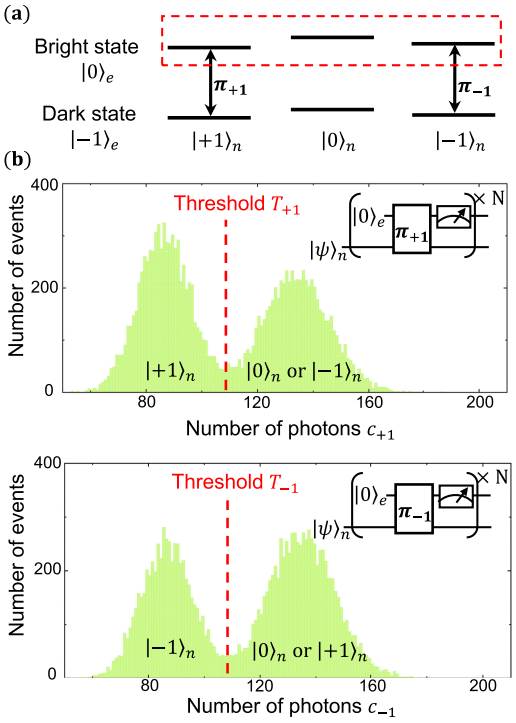

FIG. 2. Energy level of the NV center system and single-shot readouts of the nuclear spin. (a) Diagram of the states we utilized. The red dashed box encircles the energy levels that we implemented the switching process. π_{+1} and π_{-1} are selective π pulses that act on corresponding energy levels. (b) The photon counting histograms obtained by repeating the single-shot readout of $|+1\rangle_n$ (top panel) and $|-1\rangle_n$ (bottom panel). Insets are the quantum circuits. The histograms are divided into two parts by properly chosen thresholds that distinguish different nuclear spin states.

We tested the JE with a single spin-1 nuclear spin of the NV center in diamond. The NV center is a point defect in diamond that consists of an electron spin formed by the vacancy and a nuclear spin of the ^{14}N atom. The spin quantum number of both the electron spin and the nuclear spin is 1. With a static magnetic field applied along the NV symmetry axis, the ground state Hamiltonian can be written as $H_{\rm NV} = 2\pi(DS_z^2 + \omega_e S_z + PI_z^2 + \omega_n I_z + AS_zI_z)$. Here $D = 2.87$ GHz is the zero-field splitting of the electron spin, $P = -4.95$ MHz is the nuclear quadrupolar interaction constant and $A = -2.16$ MHz is the hyperfine coupling constant, ω_n (ω_e) is the Zeeman frequency of the nuclear (electron) spin. I_z and S_z are the spin-1 operators of the nuclear spin and electron spin, respectively. The energy levels we utilized are depicted in Fig. 2(a) with $|\ldots\rangle_n$ ($|\ldots\rangle_e$) encoding the nuclear (electron) spin state. The electron spin can be optically polarized to state $|0\rangle_e$ via a 532-nm laser pulse [25]. The photoluminescence (PL) rate of the NV center with the electron spin state being $|0\rangle_e$ is about 30% higher than that with the electron spin state

being $|-1\rangle_e$ [26,27]. So $|0\rangle_e$ will be denoted as the bright state and $|-1\rangle_e$ the dark state in the following. The evolution of the nuclear spin and the electron spin can be accurately manipulated via radio frequency (rf) and microwave (MW) pulses, respectively.

A test of the JE was performed on the nuclear spin of the ^{14}N atom with the electron spin state being $|0\rangle_e$. Nondemolition projective measurement of the nuclear spin is realized by cascading two high-fidelity single-shot readouts with the electron spin playing the auxiliary role. In principle, we can detect whether the nuclear spin is in one of its three possible states without altering its state by executing the single-shot readout one time [24]. The top panel of Fig. 2(b) shows the procedure of single-shot readout of $|+1\rangle_n$, which contains the following steps: (I) applying a selective MW π_{+1} pulse (optimized by gradient ascent pulse engineering algorithm [28]) to flip the electron spin from the bright state to the dark state when the nuclear spin is in $|+1\rangle_n$; (II) reading out the electron spin state via optical excitation and fluorescence collection to infer the nuclear spin state; (III) repeating (I) and (II) for N times. The photon number collected during a single run of steps (I) and (II) is not sufficient to distinguish the electron spin state, so step (III) is necessary to realize high-fidelity readout. Note that the state of the electron spin will be repolarized to the bright state after step (II) [25], which makes step (III) feasible. During the application of laser pulses in the readout process, the NV center is pumped to the excited states. The spin flip-flop processes take place and may lead to a change in the nuclear spin state. Thus, by repeating the single-shot readout to consecutively detect the nuclear spin state, we can obtain the photon-counting histogram as shown by the top panel of Fig. 2(b). The histogram contains two peaks that can be separated by an appropriate threshold (red dashed line). When the number of photons c_{+1} collected during a single-shot readout is smaller than the threshold T_{+1}, we judge the nuclear spin is in state $|+1\rangle_n$, otherwise the nuclear spin state is $|0\rangle_n$ or $|-1\rangle_n$. A single-shot readout of state $|-1\rangle_n$ can be realized by the same procedure but replace the selective MW π_{+1} pulse with π_{-1} pulse. The result is displayed in the bottom panel of Fig. 2(b). The projective measurement of the spin-1 nuclear spin was realized by cascading the single-shot readout of $|+1\rangle_n$ and $|-1\rangle_n$. Hence, the state of the nuclear spin is determined after combining the results of two comparisons between photon numbers and thresholds. The nuclear spin state is $|+1\rangle_n$ when $c_{+1} < T_{+1}$ and $c_{-1} > T_{-1}$, $|0\rangle_n$ when $c_{+1} > T_{+1}$ and $c_{-1} > T_{-1}$, and $|-1\rangle_n$ when $c_{+1} > T_{+1}$ and $c_{-1} < T_{-1}$. The events where $c_{+1} < T_{+1}$ and $c_{-1} < T_{-1}$ are excluded.

The fidelity of the single-shot readout depends on both the longitudinal relaxation time of the nuclear spin and the separation of the peaks in the photon-counting histogram. The nuclear spin state can flip during the application of 532-nm laser pulses due to the longitudinal relaxation that happens at the excited state of the NV center [29,30]. To suppress such relaxation, our experiment was implemented under a magnetic field of about 7400 G, and the direction of the magnetic field is along the NV symmetry axis [24]. With this, the longitudinal relaxation time of the nuclear spin under laser illumination was measured to be 3.8 (5) ms for $|+1\rangle_n$, 3.5 (3) ms for $|0\rangle_n$, and 4.2 (2) ms for $|-1\rangle_n$, respectively (see Sec. I of Supplemental Material [31]). The separation of the peaks can be improved by increasing the repeat time in each single-shot readout or increasing the PL rate of the NV center. But the repeat time cannot be arbitrarily increased due to the finite longitudinal relaxation time of the nuclear spin. In fact, the repeat time needs to be optimized, especially when cascading two single-shot readouts (see Sec. III of Supplemental Material for details). As for the fluorescence collection, we utilized the solid immersion lenses technology [32] and the PL rate was about 700 kps. With these methods, fidelities of 0.98(2) and 0.98(1) have been realized in making correct readouts of whether the nuclear spin state is $|+1\rangle_n$ and $|-1\rangle_n$, respectively. Based on this, high-fidelity projective measurement of the spin-1 nuclear spin can be realized, which is crucial for an experimental test of the JE (see Sec. IV of Supplemental Material for details).

In our experiment, the driving Hamiltonian during the switching process was chosen as

$$H(t) = \lambda[a(t)I_z + b(t)I_x], \tag{3}$$

where $\lambda = -\sqrt{2}\pi \times 5$ kHz, $a(t) = 1 - t/4\tau$, $b(t) = 1 - |2t/\tau - 1|$ with τ is the time duration. For the simplicity of measurement, $b(0)$ and $b(\tau)$ were set to zero. This Hamiltonian was constructed in an appropriate rotating frame by applying detuned rf pulses (see Sec. V of Supplemental Material). The thermal state of the initial Hamiltonian $H(0)$ was prepared via a series of laser, MW, and rf pulses as shown in Fig. 3(a). First, a single-shot readout was implemented to prepare the nuclear spin in state $|+1\rangle_n$ via postselection. The 532-nm laser can induce transitions between the negatively charged NV center (NV^-) and the neutrally charged NV center (NV^0) [33–35], so a 594-nm laser pulse was applied to postselect the experiment trials done with NV^- [36,37]. Then the thermal state was prepared by the following steps: (I) applying selective rf rotations $R_\theta^{+1,0}$ and $R_{\theta'}^{-1,0}$ to prepare the coherent Gibbs state [39] of $H(0)$ where $\theta = 2\arccos\sqrt{e^{-\lambda\beta}/[1+2\cosh(\beta\lambda)]}$ and $\theta' = 2\arccos\sqrt{1/(1+e^{-\lambda\beta})}$; (II) applying two selective π_{+1} pulses separated by a free evolution time $t_w = 10$ μs. t_w is about 6 times longer than the dephasing time of the electron spin [1.4(1) μs], so that the coherence between $|+1\rangle_n$ and $|0\rangle_n$ (also $|-1\rangle_n$) would be dissipated; (III) executing the similar procedure in (II) but replacing the pulse π_{+1} with π_{-1}. The coherence between $|0\rangle_n$ and $|-1\rangle_n$ can be dissipated, resulting in the nuclear spin in the thermal state of $H(0)$. The population of the initial thermal state can

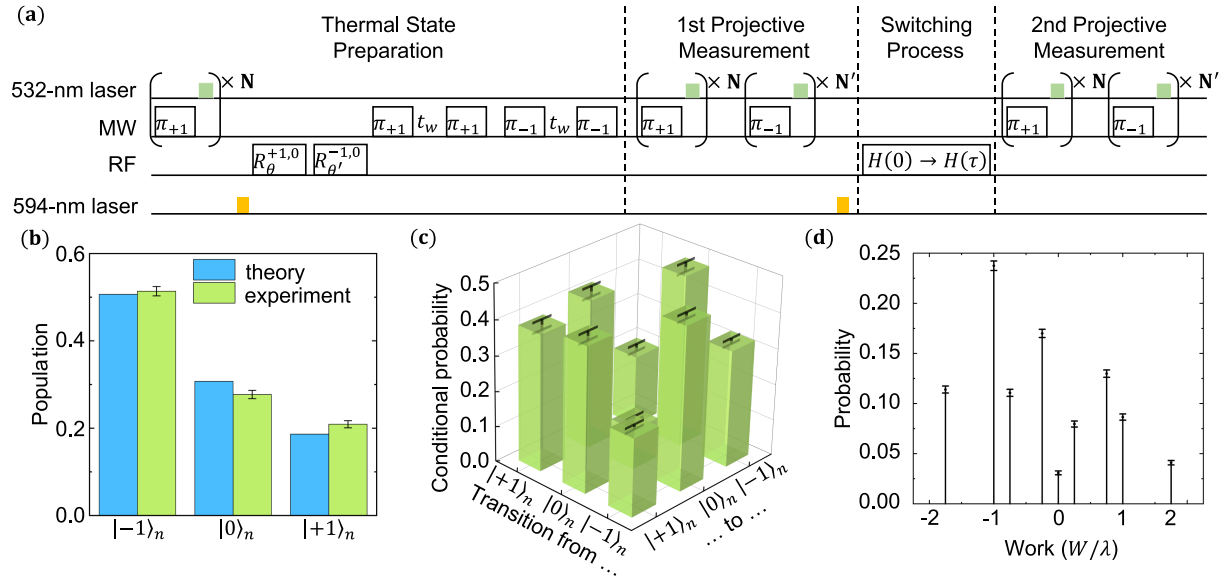

FIG. 3. Pulse sequence to test the JE and corresponding experimental results. (a) Diagram of the pulse sequence. The repeat times were set as $\mathbf{N} = \mathbf{N}' = 900$. (b) Theoretical anticipation (blue) and measured values (green) of the thermal state for $\beta|\lambda| = 0.5$. (c) The conditional probabilities obtained from the TPM protocol for $\beta|\lambda| = 0.5$ and $\tau = 200$ μs. (d) The work statistics obtained from (c). All error bars in (b)–(d) show one standard deviation.

be obtained via the first projective measurement. Figure 3(b) shows the results where the effective temperature was set as $\beta|\lambda| = 0.5$. The population of $|+1\rangle_n$, $|0\rangle_n$, and $|-1\rangle_n$ is measured to be 0.519(7), 0.276(5), and 0.204(5), respectively, yielding a fidelity of 99.82% with the theoretical anticipation and the practical inverse temperature $\beta_{\text{exp}}|\lambda| = 0.49(2)$.

We carried on the test after the thermal state was prepared by following the steps in Fig. 3(a). The nuclear spin state was in one eigenstate of $H(0)$ after the execution of the first projective measurement. Then the 594-nm laser pulse was applied again to exclude experiment trials done with NV^0. Next, detuned rf pulses were applied to construct Hamiltonian $H(t)$ and realize the switching process. Finally, the second projective measurement was performed to obtain the conditional probability $P^\tau_{m|n}$. The conditional probabilities are plotted in Fig. 3(c) by taking the switching process with $\tau = 200$ μs as an example. The diagonal elements of the bar graph represent the probabilities of the states remaining unchanged, the off-diagonal elements are the probabilities of transitions between different states. The probabilities of each trajectory are nonzero, indicating that the evolution is not adiabatic. To quantitatively illustrate the adiabaticity of the switching process, we define the adiabaticity factor [38] as

$$\mathcal{F}_A \triangleq \min_{m,n} \min_{0\le t\le\tau} \frac{(\epsilon_m^t - \epsilon_n^t)^2}{|\langle m(t)|\frac{dH}{dt}|n(t)\rangle|}, \tag{4}$$

where $|m(t)\rangle$ and $|n(t)\rangle$ are the instantaneous eigenstates of $H(t)$, ϵ_m^t and ϵ_n^t are the corresponding instantaneous eigenenergies. The switching process is adiabatic when $\mathcal{F}_A \gg 1$ and it is nonadiabatic otherwise. In the case considered here, the adiabaticity factor $\mathcal{F}_A = 1.77$, which agrees that Fig. 3(c) shows the result of a nonadiabatic process. The work distribution can be acquired from the population of the thermal state and the conditional probabilities, i.e., $P(W = W_{m|n}) = P_n^0 P_{m|n}^\tau$, and the result is shown in Fig. 3(d). With the knowledge of the work statistics, the validity of the JE can be tested. The ensemble average of the exponentiated work here is $\langle e^{-\beta W}\rangle = 0.97(1)$ and the theoretical prediction of the right-hand side of the JE is $e^{-\beta\Delta F} = 0.966(3)$. Hence, the JE is verified within the error of one standard deviation in this case.

We tested the JE at different effective temperatures. The effective inverse temperatures in Figs. 4(a)–4(c) were preset as $\beta|\lambda| = 0$, 0.5, 0.7, respectively, with $\beta|\lambda| = 0$ corresponding to infinitely high temperature and the other two representing finite ones. The practical inverse temperatures were measured to be $\beta_{\text{exp}}|\lambda| = 0.02(1)$, 0.49(2), and 0.71(2). The dots in Fig. 4 are the results of $\langle e^{-\beta W}\rangle$ and the bands show the results of the exponentiated free energy difference $e^{-\beta\Delta F}$. Both the error bar of the dots and the width of the bands display one standard deviation. All the dots are in the area covered by the bands, showing the validity of the JE under different effective temperatures.

To further investigate the universality of the JE, we carried out experiments with different switching times. The switching time was set as $\tau = 5$, 50, 125, 200, and 2500 μs. The corresponding adiabaticity factor varies from 0.04 to

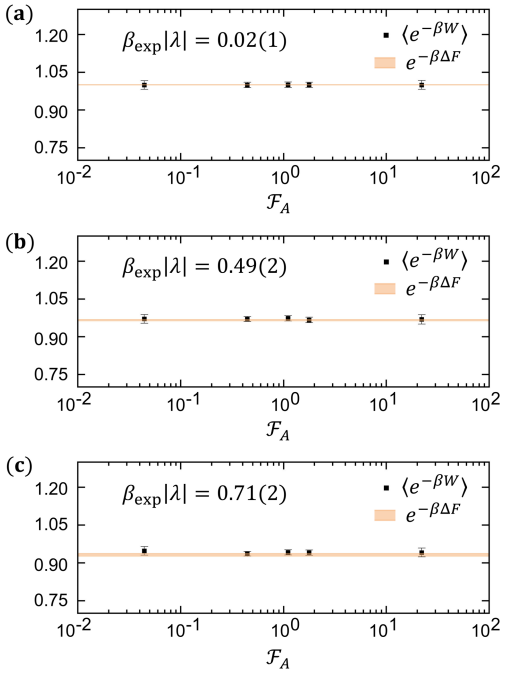

FIG. 4. Results of the JE test. The effective inverse temperatures were set as $\beta|\lambda| = 0$, 0.5, and 0.7 in (a)–(c), respectively. Practical temperatures are given in each subfigure. Black dots and orange bands show the measured values of $\langle e^{-\beta W}\rangle$ and $e^{-\beta\Delta F}$, respectively. The error bars and the width of the bands show one standard deviation.

22.09, which covers three magnitudes ranging from a nonadiabatic one to an adiabatic one. When $\tau = 5$ μs, the Hamiltonian and the corresponding energy eigenstates change rapidly, so nonadiabatic flips happen during the evolution (see Sec. VI of Supplemental Material). In contrast, the Hamiltonian and the corresponding energy eigenstates vary slowly when $\tau = 2500$ μs. The evolution of the quantum system follows the trajectory of the energy eigenstates and nonadiabatic flip barely happens. The experiment results are displayed separately in three subfigures of Fig. 4. It is found that, regardless of the time duration of the switching process, the ensemble average of the exponentiated work always equals the exponentiated difference in free energy within the margin of error. This demonstrates that the JE is valid ranging from the adiabatic region to the nonadiabatic region.

In conclusion, we tested the JE in a single spin-1 nuclear spin system. Nondemolition projective measurements of the three-level nuclear spin have been realized, which enables direct measurement of the quantum work through the standard TPM protocol. The validity of the JE was experimentally verified by tests executed at different effective temperatures and for evolutions ranging from the nonadiabatic region to the adiabatic region. Our test solidifies the crucial application of the JE in estimating the free energy difference of practical high-dimensional quantum systems, especially via fast out-of-equilibrium processes. It is noted that the high fidelity of the single-shot readout is essential for testing the JE. Infidelity, or errors in spin state readout, will lead to incorrect assessment of work and other trajectory-based physical quantities. Such an incorrect assessment becomes more devastating as the single-shot fidelity decreases, and can even obstruct the testing of the JE and other related theorems (see Sec. IV of Supplemental Material). So, our realization of high-fidelity single-shot readout makes the NV center system a promising platform to scrutinize other important thermodynamic theorems and investigate rich thermodynamic phenomena, such as the information-related JE [40–42], the Crooks fluctuation theorem [43], the generalized JE for arbitrary initial states [44,45], suppression of work fluctuation [46–48], and quantum stochastic thermodynamics with feedback involved [49–52].

We thank Yang Wu and Yunhan Wang for the helpful discussion. This work was supported by the National Key R&D Program of China (Grants No. 2018YFA0306600 and No. 2016YFB0501603), the National Natural Science Foundation of China (Grants No. 12174373, No. 61771278, and No. 12261160569), the Chinese Academy of Sciences (Grants No. XDC07000000, No. GJJSTD20200001, No. QYZDY-SSW-SLH004, and No. QYZDB-SSW-SLH005), Innovation Program for Quantum Science and Technology (Grant No. 2021ZD0302200), Anhui Initiative in Quantum Information Technologies (Grant No. AHY050000), and Hefei Comprehensive National Science Center. X. R. thanks the Youth Innovation Promotion Association of Chinese Academy of Sciences for their support. W. L. is funded by Beijing University of Posts and Telecommunications Innovation Group. Z. Y. is supported by Beijing Institute of Technology Research Fund Program for Young Scholars.

W. L. and Z. N. contributed equally to this work.

*zqyin@bit.edu.cn
†xrong@ustc.edu.cn
‡djf@ustc.edu.cn

[1] M. Esposito, U. Harbola, and S. Mukamel, Rev. Mod. Phys. **81**, 1665 (2009).
[2] M. Campisi, P. Hänggi, and P. Talkner, Rev. Mod. Phys. **83**, 771 (2011).
[3] G. T. Landi and M. Paternostro, Rev. Mod. Phys. **93**, 035008 (2021).
[4] H. B. Callen and T. A. Welton, Phys. Rev. **83**, 34 (1951).
[5] R. Kubo, J. Phys. Soc. Jpn. **12**, 570 (1957).
[6] C. Jarzynski, Phys. Rev. Lett. **78**, 2690 (1997).
[7] C. Jarzynski, Phys. Rev. E **56**, 5018 (1997).
[8] J. Liphardt, S. Dumont, S. B. Smith, I. Tinoco Jr., and C. Bustamante, Science **296**, 1832 (2002).
[9] J. Berg, Phys. Rev. Lett. **100**, 188101 (2008).

[10] F. Douarche, S. Ciliberto, A. Petrosyan, and I. Rabbiosi, Europhys. Lett. **70**, 593 (2005).
[11] V. Blickle, T. Speck, L. Helden, U. Seifert, and C. Bechinger, Phys. Rev. Lett. **96**, 070603 (2006).
[12] N. C. Harris, Y. Song, and C.-H. Kiang, Phys. Rev. Lett. **99**, 068101 (2007).
[13] G. Hummer and A. Szabo, Proc. Natl. Acad. Sci. U.S.A. **98**, 3658 (2001).
[14] O.-P. Saira, Y. Yoon, T. Tanttu, M. Möttönen, D. V. Averin, and J. P. Pekola, Phys. Rev. Lett. **109**, 180601 (2012).
[15] A. Solfanelli, A. Santini, and M. Campisi, PRX Quantum **2**, 030353 (2021).
[16] T. B. Batalhão, A. M. Souza, L. Mazzola, R. Auccaise, R. S. Sarthour, I. S. Oliveira, J. Goold, G. De Chiara, M. Paternostro, and R. M. Serra, Phys. Rev. Lett. **113**, 140601 (2014).
[17] F. Cerisola, Y. Margalit, S. Machluf, A. J. Roncaglia, J. P. Paz, and R. Folman, Nat. Commun. **8**, 1241 (2017).
[18] S. An, J.-N. Zhang, M. Um, D. Lv, Y. Lu, J. Zhang, Z.-Q. Yin, H. T. Quan, and K. Kim, Nat. Phys. **11**, 193 (2015).
[19] P. Hänggi and P. Talkner, Nat. Phys. **111**, 108 (2015).
[20] P. Talkner, E. Lutz, and P. Hänggi, Phys. Rev. E **75**, 050102(R) (2007).
[21] H. Tasaki, arXiv:cond-mat/0009244.
[22] J. Kurchan, arXiv:cond-mat/0007360.
[23] S. Mukamel, Phys. Rev. Lett. **90**, 170604 (2003).
[24] P. Neumann, J. Beck. M. Steiner, F. Rempp, H. Fedder, P. R. Hemmer, J. Wrachtrup, and F. Jelezko, Science **329**, 542 (2010).
[25] J. Harrison, M. J. Sellars, and N. B. Manson, J. Lumin. **107**, 245 (2004).
[26] F. Jelezko, T. Gaebel, I. Popa, A. Gruber, and J. Wrachtrup, Phys. Rev. Lett. **92**, 076401 (2004).
[27] M. W. Doherty, N. B. Manson, P. Delaney, F. Jelezko, J. Wrachtrup, and L. C. L. Hollenberg, Phys. Rep. **528**, 1 (2013).
[28] B. Rowland and J. A. Jones, Phil. Trans. R. Soc. A **370**, 4636 (2012).
[29] J. R. Maze, A. Gali, E. Togan, Y. Chu, A. Trifonov, E. Kaxiras, and M. D. Lukin, New J. Phys. **13**, 025025 (2011).
[30] V. Jacques, P. Neumann, J. Beck, M. Markham, D. Twitchen, J. Meijer, F. Kaiser, G. Balasubramanian, F. Jelezko, and J. Wrachtrup, Phys. Rev. Lett. **102**, 057403 (2009).
[31] See Supplemental Material at http://link.aps.org/supplemental/10.1103/PhysRevLett.131.220401 for details of experimental setup and procedures, single-shot readout, and the projective measurement, which includes Refs. [24,28–30,32–38].
[32] J. P. Hadden, J. P. Harrison, A. C. Stanley-Clarke, L. Marseglia, Y.-L. D. Ho, B. R. Patton, J. L. O'Brien, and J. G. Rarity, Appl. Phys. Lett. **97**, 241901 (2010).
[33] T. Gaebel, M. Domhan, C. Wittmann, I. Popa, F. Jelezko, J. Rabeau, A. Greentree, S. Prawer, E. Trajkov, P. R. Hemmer, and J. Wrachtrup, Appl. Phys. B **82**, 243 (2006).
[34] N. B. Manson and J. P. Harrison, Diam. Relat. Mater. **14**, 1705 (2005).
[35] G. Waldherr, J. Beck, M. Steiner, P. Neumann, A. Gali, Th. Frauenheim, F. Jelezko, and J. Wrachtrup, Phys. Rev. Lett. **106**, 157601 (2011).
[36] N. Aslam, G. Waldherr, P. Neumann, F. Jelezko, and J. Wrachtrup, New J. Phys. **15**, 013064 (2013).
[37] Y. Doi *et al.*, Phys. Rev. X **4**, 011057 (2014).
[38] T. Albash and D. A. Lidar, Rev. Mod. Phys. **90**, 015002 (2018).
[39] H. Kwon, H. Jeong, D. Jennings, B. Yadin, and M. S. Kim, Phys. Rev. Lett. **120**, 150602 (2018).
[40] V. Vedral, J. Phys. A **45**, 272001 (2012).
[41] J. M. R. Parrondo, J. M. Horowitz, and T. Sagawa, Nat. Phys. **11**, 131 (2015).
[42] D. Barker, M. Scandi, S. Lehmann, C. Thelander, K. A. Dick, M. Perarnau-Llobet, and V. F. Maisi, Phys. Rev. Lett. **128**, 040602 (2022).
[43] G. E. Crooks, Phys. Rev. E **60**, 2721 (1999).
[44] Z. Gong and H. T. Quan, Phys. Rev. E **92**, 012131 (2015).
[45] T. M. Hoang, R. Pan, J. Ahn, J. Bang, H. T. Quan, and T. Li, Phys. Rev. Lett. **120**, 080602 (2018).
[46] G. Xiao and J. Gong, Phys. Rev. E **90**, 052132 (2014).
[47] G. Xiao and J. Gong, Phys. Rev. E **92**, 022130 (2015).
[48] K. Funo, J.-N. Zhang, C. Chatou, K. Kim, M. Ueda, and A. del Campo, Phys. Rev. Lett. **118**, 100602 (2017).
[49] G. Manzano, F. Plastina, and R. Zambrini, Phys. Rev. Lett. **121**, 120602 (2018).
[50] Y. Masuyama, K. Funo, Y. Murashita, A. Noguchi, S. Kono1, Y. Tabuchi, R. Yamazaki, M. Ueda, and Y. Nakamura, Nat. Commun. **9**, 1291 (2018).
[51] M. Naghiloo, J. J. Alonso, A. Romito, E. Lutz, and K. W. Murch, Phys. Rev. Lett. **121**, 030604 (2018).
[52] T. Yada, N. Yoshioka, and T. Sagawa, Phys. Rev. Lett. **128**, 170601 (2022).